

# BER Performance Analysis of MIMO-OFDM Communication Systems Using Iterative Technique Over Indoor Power Line Channels in an Impulsive Noise Environment

Mohammad Reza Ahadiat\*

Department of Electrical Engineering, Mehriz Branch, Islamic Azad University, Yazd, Iran  
m.ahadiat@srbiau.ac.ir

Paeiz Azmi

Department of Electrical and Computer Engineering, Tarbiat Modares University, Tehran, Iran  
pazmi@modares.ac.ir

Afroz Haghbin

Department of Electrical Engineering, Science and Research Branch, Islamic Azad University, Tehran, Iran  
ahaghbin@gmail.com

Received: 02/Dec/2014

Revised: 16/Aug/2015

Accepted: 23/Aug/2015

## Abstract

This paper addresses the performance of MIMO-OFDM communication system in environments where the interfering noise exhibits non-Gaussian behavior due to impulsive phenomena. It presents the design and simulation of an iterative technique that aims to minimize the effect of impulsive noise on the performance of the MIMO-OFDM communication system under Additive White Gaussian Noise (AWGN) channel. This is a new method to recover the signals corrupted by impulsive noise in MIMO-OFDM systems over In-home Power Line Channel. The location and amplitude Impulsive noise at the receiver using an adaptive threshold to be determined. Reduced Impulsive noise effects using the mask based on the soft decision method. By iteration, the original signal estimation can be used to improve the impulsive noise estimation. This continuous loop impulsive noise detection and mitigation a better estimate of the original signal is obtained. The Bit Error Rate (BER) performance of the MIMO-OFDM system in an impulsive noise environment was evaluated. The results show the superiority and robustness of the proposed method.

**Keywords:** Power Line Communication; MIMO; OFDM; Impulsive Noise; Iterative Method.

## 1. Introduction

The Power Line Communication (PLC) is a communication protocol that uses electrical wiring to simultaneously carry both data, and Alternating Current electric power transmission or electric power distribution. PLC networks can be divided into in-home network and out-home according to their applications. The applications of PLC in-home network have been increasing recently due to the development of Home Plug power line Alliance, which has published its standard, HomePlug specification [1]. Digital communication systems over power line channel suffer from several disturbances. Such the disturbances are composed of colored gaussian noise, impulsive noise, channel interference, frequency selective fading, attenuation, and so on[2,3].

Orthogonal Frequency Division Multiplexing (OFDM) modulation schemes is a promising technique being used for bandwidth efficient communication over the PLC, full capacity of the channel, high-speed data services broadband, reduce the complexity equalization, its capacity to minimize Intersymbol Interference (ISI), and powerful in impulsive noise environments. It is also a strong candidate as a modulation scheme the performs better than single-carrier and spread spectrum modulation

methods. OFDM minimizes the effects of multipath and provides high robustness against selective fading. In PLC, the reliability of transmission is strongly influenced by the non-Gaussian impulsive noise. In OFDM, the Inverse Discrete Fourier Transform (IDFT) is used for modulating a block of  $N$  information symbols on  $N$  subcarriers[4]. The time duration of an OFDM symbol is  $N$  times larger than that of a single carrier system. This longer duration of OFDM symbol provide an advantage that the impulsive noise energy is spread among the  $N$  subcarriers due to the IDFT operation. This spreading causes less interference over all  $N$  subcarriers[5]. However, when the impulsive noise energy exceeds a certain threshold, a significant performance loss can occur due to the higher level of interference at each subcarrier[6]. It was shown in [7] that impulsive noise leads to an enormous loss in the capacity, as well as in the error rate performance.

Current high speed PLC technologies such as Hom plug AV uses as Single-Input Single-Output (SISO) communication mode and provides usable application level throughputs on typical PLC channels of about 100 Mbps. Today's in-home power line channel for 3-wire installations (phase, neutral and protective earth) basically allow more feeding and receiving possibilities, which is the precondition to apply Multiple-Input Multiple-Output

\* Corresponding Author

(MIMO) and Alamouti coding methods[8]. In [9] the suitability of MIMO for in-home PLC has been investigated. It has been shown that MIMO can significantly increase the bit rate. Typically it is more than doubled compare to today's SISO systems. Alamouti scheme is considered to be the best choice of different MIMO schemes in the PLC environment. The advantages of the MIMO-PLC system mainly lies in namely increased channel capacity and reduced BER[10]. MIMO techniques in combination with orthogonal frequency-division multiplexing (MIMO-OFDM) have been identified as a promising approach for high spectral efficiency wide band systems.

Different methods based on OFDM for reducing impulsive noise over SISO in-home power line channels have been proposed. The performance of these methods, depends on the number of sub-carriers. For a large number of sub-carriers the convergence speed is fast, whereas, for a small number of sub-carriers the algorithms converge slowly or even not at all. For a small number of sub-carriers, the noise components after Discrete Fourier Transform (DFT) have an impulsive distribution. To compensate for the limitations of these systems and to be able to adopt it for all sub-carriers, a new adaptive iterative method is proposed in this work. Using this method, smaller number of iterations are needed, the impulsive noise is reduced and a better performance is achieved.

At the receiver, after ZFE, impulsive noise detection algorithm based on adaptive threshold for estimating the impulsive noise, determines the locations and amplitudes of the impulsive noise. The adaptive threshold technique utilized is optimized radar's Constant False Alarm Rate (CFAR) detector technique [11]. After noise symbol determination, impulsive noise effect on the noise symbols is reduced using the reduction factor based on the soft decision method. The reduction factor is defined as an exponential function of the absolute difference between the estimated impulsive noises of the adaptive threshold. Then, the original signal is estimated using MLD. To improve performance, the proposed method can be repeated. By iteration, the original signal estimation can be used to improve the impulsive noise estimation. As this continuous loop impulsive noise detection and mitigation to receive together with MLD, a better estimate of the original signal is obtained.

## 2. System Model

The general model of a PLC is depicted in Fig. 1.

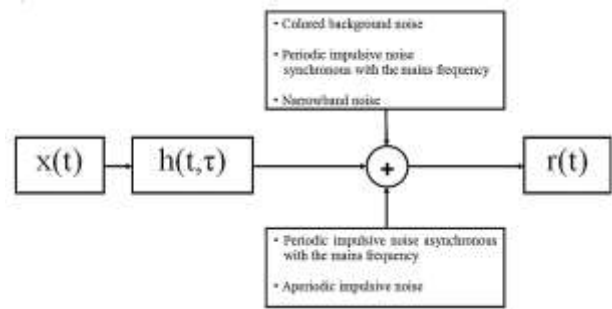


Fig. 1. Power line channel noise scenario

The  $h(t, \tau)$  is channel impulse response and is represented by a channel filter and different noise components as depicted in Fig. 1 can be expressed as background noise and impulsive noise[12].

### 2.1 Background Noise Modeling

The background noise can create disturbances in the frequency range 0-100 MHz [13]-[14]. The background noise can be separated in colored noise and narrowband interference[12]. The background noise according to [15], can be modeled in the simple three-parameter model, where the noise is considered gaussian with the Power Spectral Density (PSD) can be expressed as:

$$R_{nb}(f) = a + b|f|^c \quad \left[ \frac{\text{dBm}}{\text{Hz}} \right] \quad (1)$$

Where  $f$  is the frequency in MHz, and  $a$ ,  $b$  and  $c$  are parameters derived from measurements. The worst and best condition in-home power line channel parameter values are characterized by  $[a, b, c] = [-145, 53.23, -0.337]$  and  $[a, b, c] = [-140, 38.75, -0.72]$ , respectively, in this work. The PSD of these conditions is shown in Fig.2.

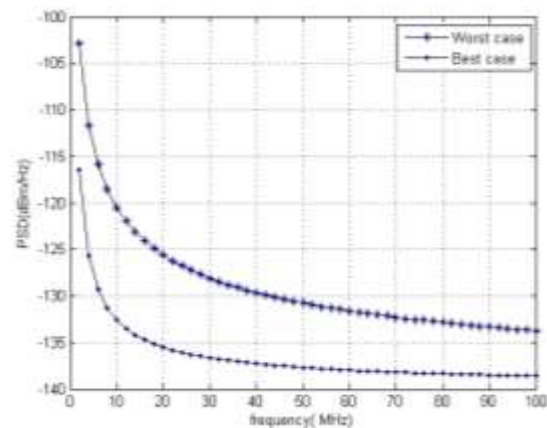


Fig. 2. The PSD of background noise for the worst and best conditions used in this work.

### 2.2 Impulsive Noise Modeling

The impulsive noise can be separated in periodic impulsive noise synchronous with the mains frequency, Periodic impulsive noise asynchronous with the mains frequency and aperiodic impulsive noise [12],[16]. Therefore, the overall noise can be written as:

$$\eta(t) = n_b(t) + n_{imp}(t) \quad (2)$$

where  $n_b(t)$  denotes the background noise, while  $n_{imp}(t)$  denotes the impulsive noise. The impulsive noise can be modeled with an arrival process. This process is specified by the statistics of the impulse amplitude  $A_{imp}$ , interarrival time  $t_{iat}$ , and duration  $t_{wid}$ . Most of the literature focuses on the statistics of the amplitude, as the Middleton's classification of electromagnetic interference [17] and the two-term gaussian mixture [18] model. The temporal characteristics have been modeled via Markov Chains in [12], Bernoulli process in [19] and curve fitting tools from experimental measurements in [15].

A relatively simple model which incorporates background noise and impulsive noise based on the Poisson Gaussian model is known as Middleton's class-A impulsive.

In the Middleton's model [17], the noise is categorized into three different types A, B and C. Because Middleton's class-A impulsive noise model is more accurate and also meets all the basic requirements in modeling the real impulsive noise, this model has been used widely in performance analysis of PLC systems. This thesis also relies on Middleton's class-A to model impulsive noise and design communications systems over power lines. Middleton's class-A model uses the Poisson Gaussian model to represent the background noise and impulsive noise. The occurrence probability of impulsive noise is modeled by a Poisson random process with the probability of having  $m$  impulsive noise events in a time interval  $T$  given by:

$$P = \frac{(\lambda T)^m e^{-\lambda T}}{m!} \quad (3)$$

The amplitudes of both background and impulsive noise are modeled by Gaussian random processes. Let  $A = \lambda T$  and call it the impulsive index. According to the Middleton's Class A noise model, the normalized complex probability density function (PDF) of the model is given by:

$$p_A(n) = \sum_{m=0}^{\infty} \frac{e^{-A} A^m}{m!} \cdot \frac{1}{\sqrt{2\pi\sigma_m^2}} \exp\left(-\frac{n^2}{2\sigma_m^2}\right) \quad (4)$$

$$\sigma_m^2 = \left( \frac{\left(\frac{m}{A}\right) + \Gamma}{1 + \Gamma} \right) \cdot \sigma^2$$

$$A \in [10^{-2}, 1], \Gamma \in [10^{-6}, 1]$$

where  $\sigma_m^2$  is the  $m$ th impulsive power,  $A$  is impulsive index,  $\sigma^2$  is total noise power (including the powers of impulsive noise and Gaussian background noise), and  $\Gamma = \frac{\sigma_G^2}{\sigma_I^2}$  is Gaussian to Impulsive noise power Ratio (GIR) with  $\sigma_G^2$  and  $\sigma_I^2$  are the powers of Gaussian and impulsive noise, respectively. When  $A$  is increased, the impulsiveness reduces and the noise comes closer to gaussian noise. Eq. (4) also shows that sources of impulsive noise have a Poisson distribution, and each impulsive noise source generates a characteristic Gaussian noise with a different variance. A good approximation of Eq.(4), is obtained by cutting off the cumulative sum after

the third term [18]. The effects of impulsive parameters  $A$  and  $\Gamma$  are illustrated in Fig. 3 and Fig. 4.

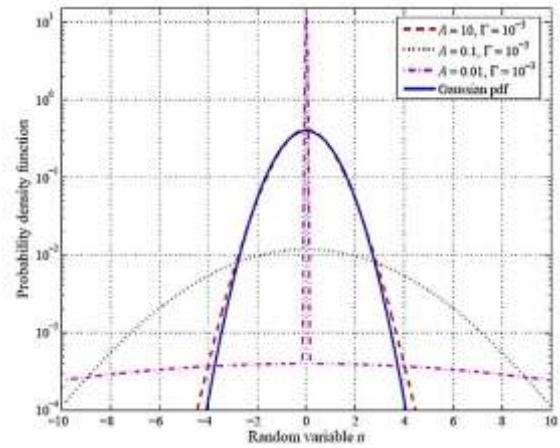


Fig. 3. Pdf of the impulsive noise with different values of impulsive index A.

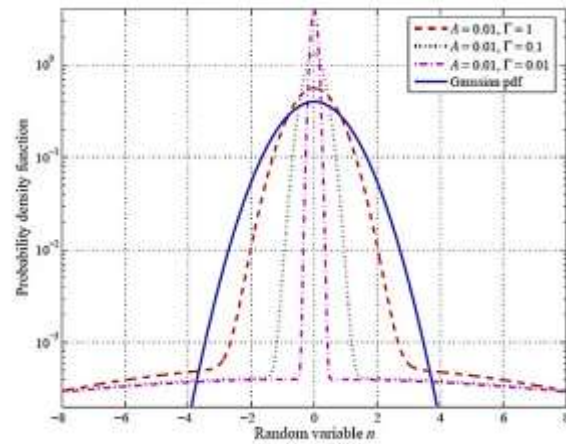


Fig. 4. Pdf of the impulsive noise with different values of  $\Gamma$

Fig. 5 also illustrate the effects of the impulsive noise parameters  $A$  and  $\Gamma$  to the amplitude distribution of class-A impulsive noise. Again, it can be seen that if  $A$  or  $\Gamma$  increases, the amplitude distribution of impulsive noise comes closer to that of Gaussian noise.

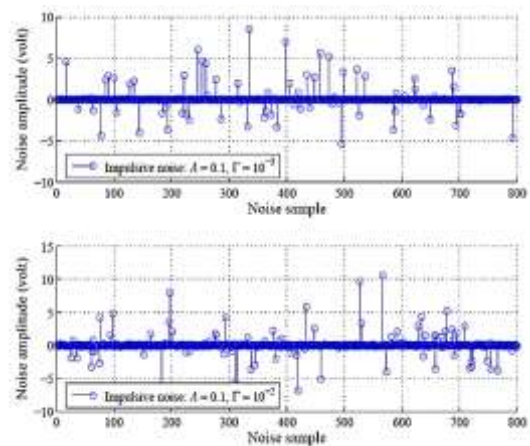


Fig. 5. Examples of impulsive noise with  $A=0.1$  and two different values of  $\Gamma$ .

### 2.3 MIMO-PLC Channel Modeling

In this paper, MIMO-PLC system which considers the coupling effects among conductors Can be modeled by Zimmermann and Dostert model[20] where the MIMO-PLC model is considered with the Channel Transfer Function (CTF) [20]:

$$H(f) = B \sum_{p=1}^{N_p} g_p(f) \cdot e^{-\alpha(f)d_p} \cdot e^{-j\left(\frac{2\pi f d_p}{v_d}\right)} \quad (5)$$

$$\alpha(f) = \text{Real}\{\alpha + j\beta = \sqrt{(R' + j\omega L')(G' + j\omega C')}\}$$

where  $N_p, B, |g_p| \leq 1, \tau_p = \frac{d_p}{v_d}, d_p, v_d = \frac{c}{\sqrt{\epsilon_r}}, \epsilon_r, \gamma,$   $\alpha$  and  $\beta$  and are the total number of fading paths, normalization term, the transmission reflection factor for path  $p$ , the  $p$ th path propagation delay, the length of the  $p$ th path, the phase velocity with  $c$  speed of light, dielectric constant, the propagation constant, the attenuation constant and the phase constant, respectively. so we are only interested in the attenuation constant. The primary cable parameters  $L'$  (inductance per unit length) and  $C'$  (capacitance per unit length) can be estimated by the geometric dimensions and the material properties. The  $R'$  (resistance per unit length) and  $G'$  (conductance per unit length) depend on frequency. The attenuation of a power line cable can be characterized by [21]:

$$A(f, d_p) = e^{-\alpha(f)d_p} = e^{-(a_0+a_1f^k)d_p} \quad (6)$$

The parameters  $a_0, a_1, K$  are chosen to adapt the model to a specific network. In this paper According to [22] a statistical model of the channel can be derived by considering the parameters in Eq. (5) as random variables. The path lengths are assumed to be drawn from a Poisson arrival process with intensity  $\Lambda$  in  $m^{-1}$ . The reflection factors  $g_p$  are assumed to be real, independent, and uniformly or log-normally distributed. Finally, the parameters  $a_0, a_1$  and  $K$  are appropriately chosen to a fixed value[23].

All PLC available today use one transmitting and one receiving port for their communication. The signal is symmetrically fed and received between the live and neutral wire. In Iran, in-home installations consist of three wires, which offers additional feeding and receiving options. Fig. 6 shows the PLC MIMO channel. Differential signaling between any two of the three wires lead to three different feeding possibilities: P (Phase or Live) to N (Neutral), P to PE (Protective Earth), and N to PE.

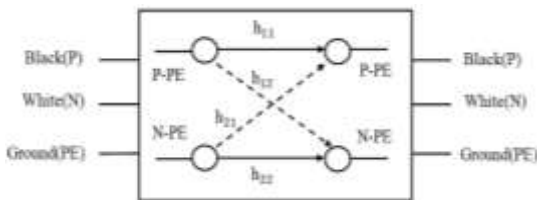


Fig. 6. In-home power line channels with two-input and two-output.

According to Kirchhoff's rule the sum of the three input signals has to be zero. Therefore only two out of the three independent input ports can be used. On receiving

side all three differential reception ports are available[8]. The coupling effects between conductors in the MIMO-PLC should be considered. The CTF in MIMO system for the  $i$ th transmit to the  $j$ th receive path (where  $i = 1, 2$  and  $j = 1, 2$ ) can be written as:

$$H_{i,j}(f) = \sum_{p=1}^{N_p} B g_p(f) \cdot e^{-\alpha_{i,j}(f)d_p} \cdot e^{-j2\pi f \tau_p} \quad (7)$$

Eq. (7) can be extended to the overall transfer function matrix:

$$H_{MIMO} = \begin{bmatrix} H_{1,1}(f) & H_{1,2}(f) \\ H_{2,1}(f) & H_{2,2}(f) \end{bmatrix} \quad (8)$$

where  $H_{i,j}, i = j$  indicate co-channels and  $H_{i,j}, i \neq j$  indicate cross channels. The attenuation constant  $\alpha_{i,j}$  in Eq. (7) can be extracted from:

$$\alpha_{i,j} = \text{real}\left\{\left(\sqrt{(R'' + j\omega L'') \cdot (G'' + j\omega C'')}\right)_{i,j}\right\} \quad (9)$$

where the operator  $\cdot$  indicates the element-wise matrix multiplication.  $R'', L'', C''$  and  $G''$  correspond to transmission line matrices[24], which represent the mutual interactions between conductors. The equivalent per-unit-length (p.u.l) parameter model [9] can be used to characterize the in-home transmission line, as shown in Fig. 7.

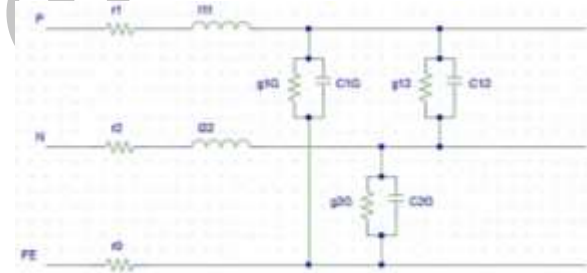


Fig. 7. The The per unit length parameter model for in-home power lines.

The resistance matrix is given as:

$$R'' = \begin{bmatrix} r_1 + r_0 & r_0 \\ r_0 & r_2 + r_0 \end{bmatrix} \quad (10)$$

where  $r_0, r_1$  and  $r_2$  are the ground resistance, the resistances for line P and the resistances for line N (which indicates line 1, line 2 in Fig. 7) per unit length, respectively and computed as:

$$r_1 = r_2 = \frac{1}{2} \sqrt{\frac{\pi f \mu_c}{\sigma_c}} \quad (11)$$

where  $\mu_c, \sigma_c$  and  $f$  and are the permeability and conductivity of conducting material, the wave frequency and, respectively. The inductance matrix is given as:

$$L'' = \begin{bmatrix} l_{11} & l_{12} \\ l_{21} & l_{22} \end{bmatrix} \quad (12)$$

where the  $l_{11}, l_{22}$  are the self-inductances for line P, N per unit length and the  $l_{12}, l_{21}$  are the mutual inductances. The computation for self-inductance per unit length is given as:

$$l_{11} = l_{22} = \frac{\mu_0}{2\pi} \ln \frac{GMD}{GMR_L}, GMD = D_{12} \quad (13)$$

Note that GMD,  $\mu_0$  and  $GMR_L$  are geometric mean distance, the permeability of dielectric material between conductors and geometric mean radian. The anti-diagonal terms in Eq.(12) can be computed as  $l_{12} = l_{21} = k\sqrt{L_{11}L_{22}}$ . where k is called the coefficient of coupling ( $0 \leq k \leq 1$ ). The capacitance matrix is given as:

$$C'' = \begin{bmatrix} c_{11} & -c_{12} \\ -c_{21} & c_{22} \end{bmatrix} \quad (14)$$

where  $c_{11}$  and  $c_{22}$  are the self-capacitances for line P, N per unit length and given as  $c_{11} = c_{1G} + c_{12}$ ,  $c_{22} = c_{2G} + c_{21}$ . and  $c_{PG}$ ,  $c_{NG}$  (i.e.,  $c_{1G}$ , or  $c_{2G}$ ) are the capacitances between line P, N and ground (G), and given as:

$$c_{1G} = \frac{2\pi\epsilon_0}{\ln \frac{GMD}{GMR_C}} \quad (15)$$

$$c_m = 4\pi\epsilon_0 (= -c_{12} = -c_{21})$$

where  $\epsilon_0$  and  $GMR_C$  are the permittivity of dielectric material between conductors and the actual conductor radius r. The conductance matrix is given as:

$$G'' = \begin{bmatrix} g_{11} & -g_{12} \\ -g_{21} & g_{22} \end{bmatrix} \quad (16)$$

$$g_{1G} = 2\pi f c_{1G} \tan \delta, \quad g_m (= -g_{12} = -g_{21})$$

where  $g_{11}$  and  $g_{22}$  are the self-conductances for line P, N per unit length and given as  $g_{11} = g_{1G} + g_{12}$ ,  $g_{22} = g_{2G} + g_{21}$ . where  $g_{PG}$ ,  $g_{NG}$  (i.e.,  $g_{1G}$  or  $g_{2G}$ ) are the conductances between line P, N and ground (G),  $\delta$  is the skin depth of the conducting material. Performing the required mathematical operation in each element of the transmission parameter matrices to solve for the attenuation factor  $\alpha_{ij}$  in Eq. (9), (i.e.,  $\alpha_{1,1} = \sqrt{(r_1 + r_0 + j\omega l_{11})(g_{11} + j\omega c_{11})}$ ,  $\alpha_{1,2} = \sqrt{(r_0 + j\omega l_{12})(g_{12} - j\omega c_{12})}$ ), the channel matrix in Eq. (10) can be obtained. [24]-[25].

## 2.4 OFDM System Modeling

Fig. 8 shows the block diagram of a MIMO-OFDM system.

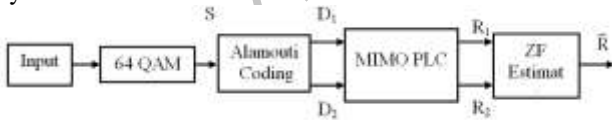


Fig. 8. Block diagram of the proposed 2\*2 MIMO-OFDM System.

In the transmitter side, input signal is first converted to digital symbol. The serial data stream of the source is mapped to data symbols with employing the signal constellation scheme of 64-QAM. Then, modulated symbols are fed to the space time block encoder [26]. Complex symbols of each transmit path are processed by OFDM modulated by an Inverse Fast Fourier Transform (IFFT) and a Cyclic Prefix (CP) insertion block. In telecommunications, the term cyclic prefix refers to the prefixing of a symbol with a repetition of the end. Although the receiver is typically configured to discard

the cyclic prefix samples, the cyclic prefix serves two purposes. The symbols are then transmitted to the receiver via a 2\*2 MIMO in-home power line channel, as shown in Fig. 6. The receiver performs the reverse operation of the transmitter. The received signal is carried out by CP removal, FFT operation. The ZF scheme applies the inverse of the frequency response of channel to the symbol received, so that the original signal can be detected to an optimum level. ZF is the one of the best linear receiver detection method having low computational complexity, but it suffers from sudden noise enhancement.

## 3. The Proposed Method

The symbols are received of 2\*2 MIMO-PLC by Alamouti scheme in OFDM-based systems over In-home Power Line Channels. The received symbols in the first time slot, and by assuming that the channel remains constant for the second time slot, the received symbols in the second time slot are:

$$\begin{aligned} R_{11} &= H_{11}S_1 + H_{12}S_2 + N_{11} \\ R_{12} &= H_{21}S_1 + H_{22}S_2 + N_{12} \\ R_{21} &= -H_{11}S_2^* + H_{12}S_1^* + N_{21} \\ R_{22} &= -H_{21}S_2^* + H_{22}S_1^* + N_{22} \end{aligned} \quad (17)$$

The received symbols are equalized by ZF equalization as shown in Fig. 9. The received symbols consist of original symbols and noises, which can be computed as:

$$R = HS + N, \tilde{S} = S + W, N, W = (H)^{\dagger} = (H^H H)^{-1} H^H \quad (18)$$

Where  $(\cdot)^{\dagger}$  is the pseudo-inverse and  $(\cdot)^H$  is the Hermitian transpose [27].

The proposed method in this paper consists of an iterative loop of three main CFAR, SOFT decision, and MLD. In this technique for impulsive noise reduction in noisy samples, of adaptive weights are used in each iteration. As depicted in Figure 6, successive detection and estimation of locations and amplitudes of impulsive noise are used to improve signal reconstruction quality [28]. For each detection and estimation step, the estimate of the noise improves using the estimated original signal from the previous step. The estimate of the impulsive noise is as follows

$$\hat{e}(n) = \hat{r}(n) - \hat{s}(n) \quad (19)$$

Where  $\hat{r}(n)$  and  $\hat{s}(n)$  are estimated received signal, and estimated original signal.

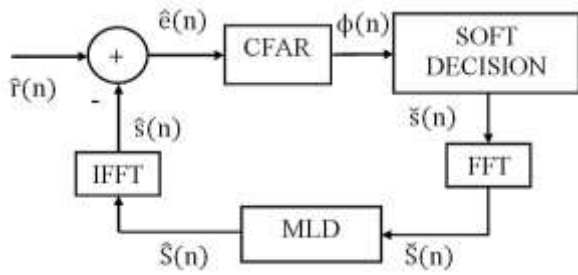


Fig. 9. Block of the proposed method.

### 3.1 Impulsive Noise Detection

The threshold in impulsive noise detection block can either be adaptive or non-adaptive. The CFAR is an adaptive threshold method used in radar detectors based on Neyman-Pearson criterion[28]. In this paper we use a Censored Mean Level (CML) CFAR. The reason we use CML-CFAR is to reduce the probability that impulses involved in averaging when number of them are present in adjacent cells. In the  $k^{\text{th}}$  order CML-CFAR of length  $2n_c$ , among the  $2n_c$  adjacent cells,  $k$  of the smallest amplitudes are averaged and the other  $2(n_c - k)$  samples (which may contain impulsive noises) are ignored. In this method, the probability of impulsive noise presence in averaged adjacent samples is reduced. To calculate adaptive thresholds in the  $m^{\text{th}}$  cell,  $2N_c$  points are expressed as  $\{n_1, \dots, n_{2N_c}\} = \{m - N_c, \dots, m + N_c\}$ , and the impulsive noise estimate in these points is sorted by the largest amplitudes  $|\hat{e}[n_1]| \leq \dots \leq |\hat{e}[n_{2N_c}]|$ . Adaptive threshold can be computed as:

$$\eta[m] = \frac{1}{k} \sum_{i=1}^k |e[n_i]| \quad (20)$$

### 3.2 Attenuation of Impulsive Noise

The detection algorithm is not an error free process in the early detection and estimation steps, especially when the amplitudes of the impulsive noises are small compared to the samples of the signal amplitudes. When the hard decision method is employed, the modulus is either zero or one at each sample. So that some samples are erased. One of the disadvantages of the soft method is its low convergence rate even when good estimates of the impulsive noise locations are available. To overcome this problem, at each stage of the detection and estimation we gradually change the soft decision to the hard decision. Simulation results for different modes suggested that the modulus function is as follows:

$$\emptyset(e[k], \eta[k]) = \exp(-\alpha|e[k] - \eta[k]|) \quad (21)$$

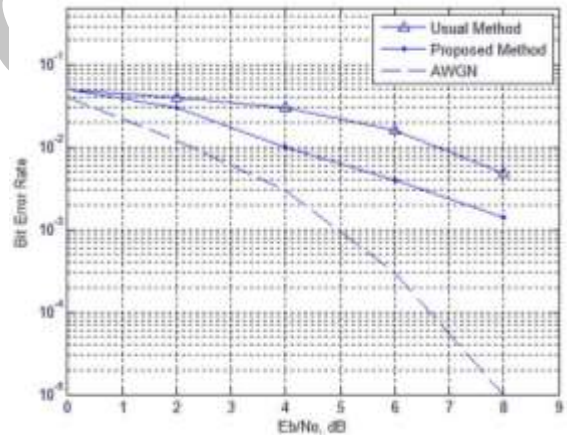
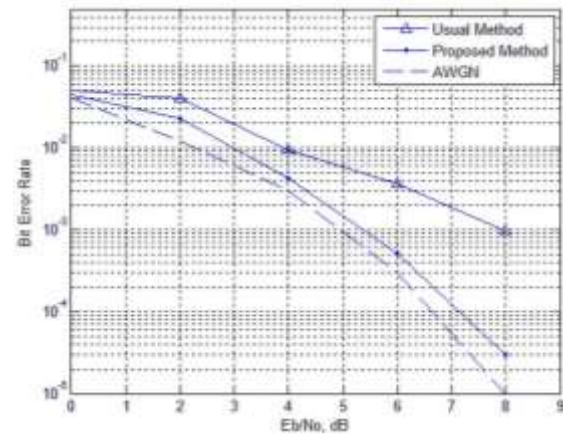
where  $\hat{e}$ ,  $\eta$  and  $\alpha$  are the estimated error, the threshold generated by CFAR [29] and the softness order of the soft decision, respectively. The suggested modulus function, the value  $e[k] - \eta[k]$  tends to zero, and then the  $\alpha$  value is increased gradually through detection and estimation steps as the convergence rate increases. In each detection and estimation step, a new mask is obtained by

$$\check{s}(n) = \hat{r}(n)\emptyset(n) = \hat{r}(n)e^{-\alpha|\hat{e}(n)-\eta(n)} \quad (22)$$

## 4. Simulation Results

To evaluate the proposed method, OFDM modulation with 64 sub-carriers together with *Alamouti coding* to transmit, and  $2 \times 2$  In-home PLC, and CFAR, Soft Decision with MLD to receive are simulated. It is assumed OFDM with a small number of sub-carriers that all sub-carriers are used for data transmission (not be used for pilot tones) and  $10^4$  symbols ( $5 \times 10^6$  bits), the impulsive noise from Middleton's class-A model is generated, and the noise samples are independent and identically distributed (i.i.d). According to the proposed MIMO model for in-home power line channels, and power line characteristics, parameters of (10) were calculated [31].

Fig. 10 and Fig. 11 shows the BER performance of the proposed method is compared with usual method without and with 15 iteration in power line channel, respectively. The noise on the power line channel between Gaussian noise and impulsive noise is changing. This noise is the Worst mode for impulsive noise with high range and number of impulse and is in the best state for Gaussian noise. Figure 12 shows the proposed method with the usual method performance in the worst case channel noise.

Fig. 10. Comparison of BER performance of OFDM-PLC without iteration (Impulsive Noise  $\Gamma = 0.01$ ,  $A = 0.1$ ).Fig. 11. Comparison of BER performance of OFDM-PLC with 15 iteration (Impulsive Noise = 0.01,  $A = 0.1$ ).

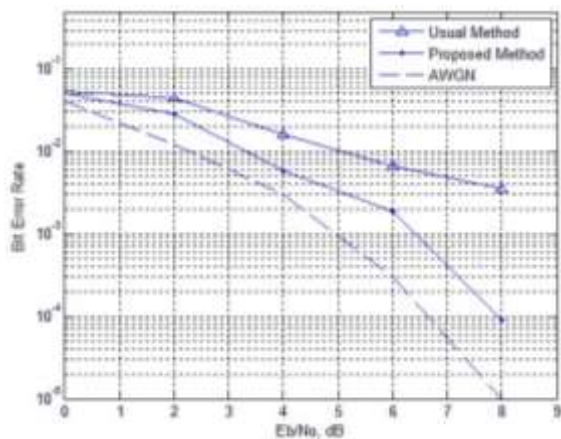


Fig. 12. Comparison of BER performance of OFDM-PLC with 15 iterations (Impulsive Noise  $\Gamma = 0.0001$  and  $A = 0.01$ ).

The best BER performance of impulsive noise reduction algorithms based on OFDM, Nonlinear Estimation and Mitigation algorithm in [32,33] and Sparse Bayesian Learning method for estimation and mitigation without training in [34] has been reported. Both of these algorithms are based on iteration. These OFDM algorithms with 64 sub-carriers are simulated. According to Fig. 13, with the same number of iterations them with proposed method are compared. Fig. 14 shows the BER performances of the proposed algorithms, for the worst case channel noise, impulsive noise with strong impulsiveness.

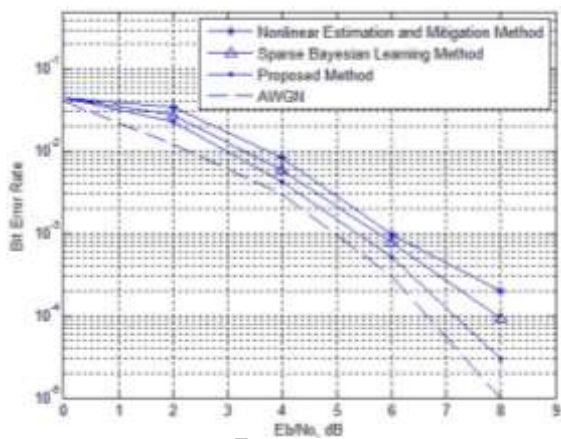


Fig. 13. The BER performance the Usual Method in comparison with the Proposed method of OFDM-PLC with 15 iterations (Impulsive Noise  $\Gamma = 0.01$  and  $= 0.1$ ).

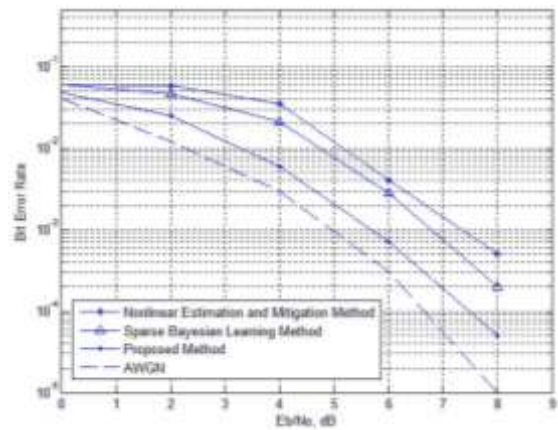


Fig. 14. The BER performance the Usual Method in comparison with the Proposed method of OFDM-PLC with 15 iterations (Impulsive Noise  $\Gamma = 0.0001$  and  $= 0.01$ ).

## 5. Conclusions

In this paper, we proposed an Impulsive Noise Estimation and Suppression in OFDM-MIMO Systems over In-home Power Line Channels. The proposed method in this paper consists of an iterative loop of three main CFAR, SOFT DECISION, and MLD. The location and amplitude Impulsive noise at the receiver using an adaptive threshold to be determined. Reduced Impulsive noise effects using the mask based on the soft decision method. By iteration, the original signal estimation can be used to improve the impulsive noise estimation. This continuous loop impulsive noise detection and mitigation a better estimate of the original signal is obtained. Simulation results show that the BER performance of proposed method was higher than the other impulsive noise estimation and mitigation methods.

## References

- [1] S. Gardner. "The HomePlug for powerline in home networking." Proc. Int. Symp. Power Line Commun. and Its Appl, pp. 67-72, 2001.
- [2] J. A. Cortes, L. Diez, F. J. Canete, J. J. Sanchez-Martinez. "Analysis of the Indoor Broadband Power-Line Noise Scenario". IEEE Trans. Electromagn. Compat, vol. 52, pp. 849-858, Nov. 2010.
- [3] M. Ghosh. "Analysis of the effect of impulse noise on multicarrier and single carrier QAM systems". IEEE Trans. Commun, vol. 44, pp. 145-147, 1996.
- [4] S. Dihan, P. Farka. "Impulsive noise cancellation in systems with OFDM modulation". Journal of Electrical Engineering, vol. 59, pp. 310-316, 2008.
- [5] H. Nikookar, D. Nathoeni. "Performance evaluation of OFDM transmission over impulsive noisy channels". IEEE. Int. Symp. Personal. Indoor and Mobile Radio Communications, vol. 2, pp. 550 - 554, Sep. 2002.
- [6] U. Epple, D. Shutin, M. Schnell. "Mitigation of Impulsive Frequency-Selective Interference in OFDM Based

- Systems". *International Journal of Scientific & Engineering Research*, vol. 4, pp. 2253-2256, May. 2013.
- [7] Y. H. Ma, P. L. So, E. Gunawan. "Performance Analysis of OFDM Systems for Broadband Power Line Communications Under Impulsive Noise and Multipath Effects". *IEEE Trans. Power Delivery*, vol. 20, pp. 674-682, Apr. 2005.
- [8] L. Hao, J. Guo. "A MIMO-OFDM Scheme over Coupled Multi-conductor Power-Line Communication Channel." *IEEE. Int. Symp. Power Line Commun. and Its Appl*, pp. 198-203, 2007.
- [9] L. Stadelmeier, D. Schneider, D. Schill, A. Schwager, J. Speidel. "MIMO for In-home Power Line Communications." in *International Conference on Source and Channel Coding (SCC)*.Ulm, pp. 1-6, Jan. 2008.
- [10] A. Canova, N. Benvenuto, P. Bisaglia. "Receivers for MIMO-PLC channels: Throughput comparison." *IEEE. Int. Symp. Power Line Commun. and Its Appl*, pp. 114-119, Mar. 2010.
- [11] M. Skolnik. *Introduction to Radar Systems*: McGraw-Hill, 2000, pp. 126-140.
- [12] M. Zimmermann, K. Dostert, "An analysis of the broadband noise scenario in powerline networks." *IEEE. Int. Symp. Power Line Commun. and Its Appl*, pp. 131-138, Apr. 2000.
- [13] H. Philipps, "Performance measurements of power line channels at high frequencies." *IEEE. Int. Symp. Power Line Commun. and Its Appl*, pp. 229-237, Mar. 1998.
- [14] B. Praho, M. Tlich, P. Pagani, A. Zeddani, F. Nouvel. "Cognitive detection method of radio frequencies on power line networks." *IEEE. Int. Symp. Power Line Commun. and Its Appl*, pp. 225-230, Mar. 2010.
- [15] T. Esmailian, F. R. Kschischang, P. G. Gulak. "In-building power lines as high-speed communication channels: Channel characterization and a test channel ensemble". *International Journal of Communication Systems*, vol. 16, pp.381-400, 2003.
- [16] A. K. S. Al-Bayati, O. M. Aloquili, J. I. AlNabulsi, "Efficient use of DS/CDMA signals for broadband communications over power lines". *International Journal of Communication Systems*, vol. 26, pp.212-221, Sep. 2011.
- [17] D. Middleton. "Statistical-physical models of electromagnetic interference." *IEEE Transactions on Electromagnetic Compatibility*, vol. 19, pp.106-127, 1977.
- [18] R. S. Blum, Y. Zhang, B. M. Sadler, R. J. Kozick. "Time-domain equalizer for multicarrier systems in impulsive noise". *International Journal of Communication Systems*, vol.25, pp.111-120, Apr. 2011.
- [19] H. Dai, H. V. Poor. "Advanced signal processing for power line communications". *IEEE Communications Magazine*, vol. 41, pp.100-107, 2004.
- [20] M. Zimmermann, K. Dostert. "A multipath model for the powerline channel". *IEEE Transactions on Communications*, vol. 50, pp.553-559, 2002.
- [21] A. M. Tonello, S. D'Alessandro, L. Lampe. "Bit, tone and cyclic prefix allocation in OFDM with application to in-home PLC." *Proc. IEEE IFIP Wireless Days Conference*, pp. 23-27, Nov. 2008.
- [22] A. M. Tonello. "Wideband Impulse Modulation and Receiver Algorithms for Multiuser Power Line Communications". *EURASIP Journal on Advances in Signal Processing*, vol. 2007, Dec. 2007
- [23] A. M. Tonello, F. Versolatto. "Bottom-up statistical PLC channel modeling—Part I: Random topology model and efficient transfer function computation". *Power Delivery. IEEE Transactions on*, vol. 26, pp.891-898, Apr. 2011.
- [24] R. Clayton, R. Paul. *Analysis of Multiconductor Transmission Lines*, John Wiley and Sons, Inc, 2004, pp. 46-62.
- [25] J. Glover, M. Sarma, T. Overbye. *Power System Analysis and Design (Fourth Edition)*, Thomson, 2008, pp. 155-213.
- [26] C. L. Giovaneli, B. Honary, P. G. Farrell. "Space-frequency coded OFDM system for multi-wire power line communications." *IEEE. Int. Symp. Power Line Commun. and Its Appl*, pp. 191-195, Apr. 2005.
- [27] P. Ferreira. "Stability issues in error control coding in the complex field, interpolation, and frame bounds." *Signal Processing Letters, IEEE*, vol. 7, pp. 57-59, 2000.
- [28] J. C. Chang, F. B. Ueng. "Performance of OFDM-CDMA receivers with MIMO communications." *International Journal of Communication Systems*, vol. 27, pp. 732-749, May. 2014.
- [29] Y. C. Tan, N. B. Ramlı. "Time-domain equalizer for multicarrier systems in impulsive noise." *International Journal of Communication Systems*, vol. 25, pp. 111-120, Feb. 2012.
- [30] S. Zahedpour, M. Ferdosizadeh, F. Marvasti, G. Mohimani, M. Babaie-Zadeh. "A novel impulsive noise cancellation based on successive approximations." in *Proceedings of SampTa 2007*, pp. 126-131, Jun. 2007.
- [31] B. Adebisi, S. Ali, B. Honary. "Space frequency and space time frequency M3FSK for indoor multi wire communication". *IEEE Trans. on Power Delivery*, vol. 24, pp. 2361-2367, Oct. 2009.
- [32] Y. C. Hsiao. "Iterative Interference Cancellation for OFDM Signals With Blanking Nonlinearity in Impulsive Noise Channels". *IEEE Signal Processing Letters*, vol. 19, pp. 147-150, Mar. 2012.
- [33] R. Sukanesh, R. Sundaraguru. "Mitigation of Impulse Noise in OFDM Systems". *Journal of Information & Computational Science*, vol. 8, pp. 2403-2409, 2011.
- [34] J. Lin, M. Nassar, L. Brian, E. Fellow. "Impulsive Noise Mitigation in Power line Communications Using Sparse Bayesian Learning". *IEEE Journal on Selected Areas of Communications*, pp. 1-26, Mar. 2013.

**Mohammad Reza Ahadiat** received the B.Sc, M.Sc, and Ph.D degrees in electrical engineering from Yazd University, Yazd, Iran, Tarbiat Modares University, Tehran, Iran, and Science and Research Branch, Islamic Azad University, Tehran, Iran, in 1999, 2003, and 2013, respectively. He is currently with the electrical and computer department of Mehriz Branch in Islamic Azad University, Yazd, Iran, as assistant professor. His areas of research include MIMO wireless communications, Power Line Communication, multicarrier modulation and estimation theory.

**Paeiz Azmi** was born in Tehran-Iran, on April 17, 1974. He received the B.Sc, M.Sc, and Ph.D degrees in electrical engineering from Sharif University of Technology (SUT), Tehran-Iran, in 1996, 1998, and 2002, respectively. Since September 2002, he has been with the Electrical and Computer Engineering Department of Tarbiat Modares University, Tehran-Iran, where he became an associate professor on January 2006 and he is a full professor now. Prof. Azmi is a senior member of IEEE. From 1999 to 2001, Prof. Azmi was with the Advanced Communication Science Research Laboratory, Iran Telecommunication Research Center (ITRC), Tehran, Iran. From 2002 to 2005, he was the Signal Processing Research Group at ITRC.

**Afroz Haghbin** received her B.Sc degree in electrical engineering from Sharif University of Technology, Tehran, Iran, in 2001. She received her M.Sc degree from Tehran University and her Ph.D degree from Tarbiat Modares University, Tehran, Iran, all in electrical engineering in 2004 and 2009, respectively. She is currently with the electrical and computer department of Science and Research Branch in Azad University, Tehran, Iran, as assistant professor. Her research interests include MIMO wireless communications, channel coding, precoding, multicarrier modulation and estimation theory.